

We can define the molecule's location to be $z = 0$, and the surface of the slab to be located at $z = D$. The total interaction potential energy can be expressed as:

$$V_{mol-surf} = \sum \frac{C_w}{d^6} \quad (1.22)$$

which sums over the energies for the molecule at $z = 0$ interacting with each molecule in the slab. To sum up the relevant interaction potentials, we can first consider the interaction potential between the molecule and a circular cross-section of the slab with a radius, r . The total number of molecules in a ring is given by:

$$\text{total \# molecules} = \rho(2\pi r)drdz \quad (1.23)$$

This distance between the molecule and each point in the slab is given by

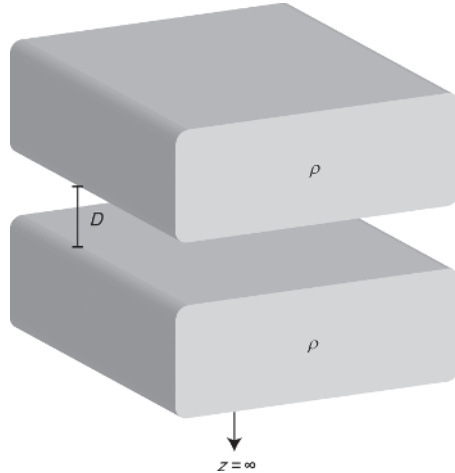
$$d = (r^2 + z^2)^{1/2}$$

such that the total interaction potential can be expressed as the integral:

$$\begin{aligned} V_{mol-surf} &= -2\pi\rho C_w \int_{z=D}^{z=\infty} \int_{r=0}^{r=\infty} \frac{rdrdz}{(r^2 + z^2)^3} \\ &= \pi\rho C_w \int_{z=D}^{z=\infty} \left[\frac{dz}{2(r^2 + z^2)^2} \right]_{r=0}^{r=\infty} \\ &= \pi\rho C_w \int_{z=D}^{z=\infty} \frac{dz}{2z^4} \\ &= \pi\rho C_w \left[\frac{1}{6z^3} \right]_{z=D}^{z=\infty} \\ &= \frac{-\pi\rho C_w}{6D^3} \end{aligned} \quad (1.24)$$

We can use the derived expression for $E_{mol-surf}$ to calculate the interaction potential for two parallel surfaces (Figure 1.26) composed of the same material:

Figure 1.26 Surface-surface interaction.



by summing over all the molecules on the second surface. Because the interaction energy between two infinite surfaces would itself be infinite, we can instead

calculate the interaction energy, $V_{surf-surf}$, per unit area. We then solve for the following expression:

$$\begin{aligned}
 V_{surf-surf} &= -\pi \rho^2 C_w \int_{z=D}^{z=\infty} \frac{dz}{6z^3} \\
 &= \left[\frac{-\pi \rho^2 C_w}{12z^2} \right]_{z=D}^{z=\infty} \\
 &= \frac{-\pi \rho^2 C_w}{12D^2} \text{ per unit area}
 \end{aligned} \tag{1.25}$$

From our above derivation, we can see the important consequence of summing vdW pair potentials: the interaction energy for larger objects composed of condensed phases decays much more slowly than for individual atoms and molecules. In this case, the interaction energy for two slabs with infinite thickness decays as $\propto 1/D^2$, compared to the $\propto 1/D^6$ scaling law exhibited for two molecules. We typically characterize the strength of an interaction based on this decay length: if a force is *short-range*, it will act on an object at separation distances <1 nm, or near contact. On the other hand, a *long-range* force can act on an object at considerable distances >1 nm. Thus, we can readily see how additive vdW forces can be sufficiently long-range when describing the interactions between nanomaterials.

Worked Example 1.11

Question: Derive an expression for the total vdW interaction energy between two parallel molecular chains (e.g. two linear polymers) that possess a linear density, σ , chain length, L , and are separated by a short distance, D (Figure 1.27).

Answer: Since two infinitely long chains will possess an infinite interaction energy, we must solve for this expression in terms of chain length, L . To start, we first sum over all of the interaction between one molecule in chain A with all of the molecules in chain B. We can define the x -axis along the length of chain B and the z -axis orthogonal to the two chains (Figure 1.27).

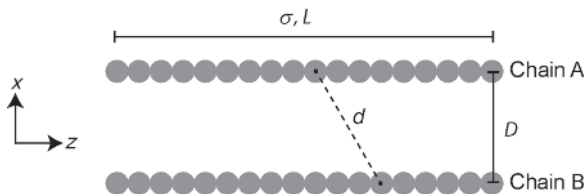


Figure 1.27 Interaction between two long chains (A and B) with separation distance, D .

The distance, r , between the molecule in chain A with those in chain B is given by:

$$d = (x^2 + z^2)^{1/2}$$

and the total number of molecules in chain B with a segment of length dx is given by:

$$\text{total \# molecules} = \frac{dx}{\sigma}$$

Thus, integrating each molecule–molecule pair potential over the entire length of chain B gives the integral:

$$\begin{aligned} V_{\text{mol-chain}} &= \int_{x=-L/2}^{x=L/2} \frac{-C_w dx}{\sigma d^6} \\ &= \frac{-2C_w}{\sigma} \int_{x=0}^{x=L/2} \frac{dx}{(x^2 + D^2)^3} \end{aligned}$$

Solving for this integral requires some extensive trigonometric substitution (a computer will help here!), but we end up with final expression:

$$V_{\text{mol-chain}} = \frac{-2C_w}{\sigma} \left[\frac{5D^3x + 3(x^2 + D^2)^2 \tan^{-1}\left(\frac{x}{D}\right) + 3Dx^3}{8D^5 (x^2 + D^2)^2} \right]_{x=0}^{x=L/2}$$

We can approximate this expression for the typical polymer case where $L \gg D$ to get:

$$\begin{aligned} V_{\text{mol-chain}} &= \frac{-2C_w}{\sigma} \left[\frac{5}{D^2 L^3} + \frac{3 \tan^{-1}\left(\frac{L}{2D}\right)}{8D^5} + \frac{3}{D^4 L} \right] \\ &= \frac{-C_w}{\sigma} \frac{3\pi}{8D^5} \end{aligned} \quad (1.26)$$

To obtain the interaction energy between the two chains, we then integrate the pair potentials for each molecule along the length of chain A:

$$\begin{aligned} V_{\text{chain-chain}} &= \frac{2}{\sigma} \int_{x=0}^{x=L/2} \frac{-C_w}{\sigma} \frac{3\pi}{8D^5} dx \\ &= \frac{-3\pi C_w}{8\sigma^2} \frac{L}{D^5} \end{aligned} \quad (1.27)$$

The constants in the expression for $V_{\text{surf-surf}}$ can be more generally expressed as:

$$A = -\pi \rho_A \rho_B C_w \quad (1.28)$$

for two interacting bodies with densities ρ_A and ρ_B , respectively. A is known as the *Hamaker constant*, named after the scientist who derived the theory describing vdW forces between macroscopic objects. The Hamaker constant is characteristic for an interacting pair of particles within a given medium. In vacuum, the Hamaker constant for most molecules and materials varies between 10^{-20} and 10^{-19} J, with hydrocarbons at the low end of these values ($0.01\text{--}5 \times 10^{-20}$ J) and metals at the high end ($15\text{--}45 \times 10^{-20}$ J). Table 1.2 lists some general values of the Hamaker constants for some common materials in vacuum. The Hamaker constant is convenient when describing the vdW interaction potentials between objects with different shapes, for which expressions can be derived by additive pair potentials. For example, using a similar approach to the previous worked example, the following expression can be derived for a sphere approaching a surface composed of the same material:

$$V(D)_{\text{sphere-surf}} = \frac{-AR}{6D} \quad (1.29)$$

Table 1.2 Hamaker constants used to calculate the energies between interacting bodies composed of the material listed, in vacuum.

| Material | Hamaker constant (10^{-20} J) |
|--------------------------------|----------------------------------|
| Au | 45.5 |
| Ag | 40.0 |
| Cu | 28.4 |
| Si | 25.6 |
| Ge | 30.0 |
| Al ₂ O ₃ | 15.5 |
| TiO ₂ (anatase) | 19.7 |
| TiO ₂ (rutile) | 31.1 |
| CdS | 15.3 |
| SiO ₂ | 16.4 |
| Graphite | 47 |
| Diamond | 28.4 |
| Water | 4.4 |
| Decane | 5.0 |
| Polystyrene | 6.2 |
| Polyvinyl alcohol | 8.8 |

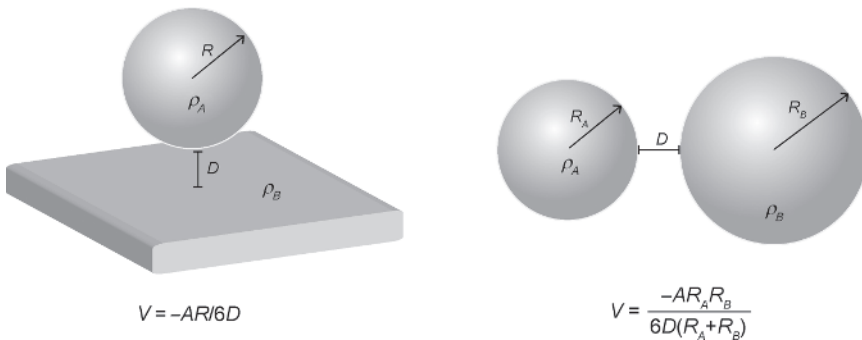
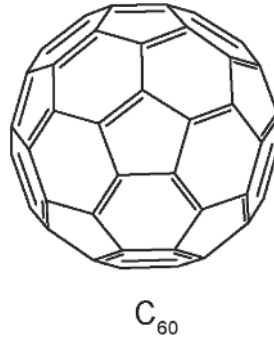


Figure 1.28 Sphere-surface and sphere-sphere interaction potentials.

where R is the radius of the sphere and D is the surface-to-surface separation distance. Similarly, we can derive an expression for two approaching spheres composed of the same material:

$$V(D)_{\text{sphere-sphere}} = \frac{-AR_A R_B}{6D(R_A + R_B)} \quad (1.30)$$

where R_A and R_B are the radii of the spheres. Figure 1.28 depicts these two pairwise geometries which are commonly found in nanoscale systems.

Figure 1.29 C_{60} molecule.**Worked Example 1.12**

Question: Shown in Figure 1.29, C_{60} condenses into solid with a density of 1.65 g/cm^3 at room temperature. Molecular C_{60} possesses a polarizability of $76.5 \times 10^{-30} \text{ m}^3$, a dipole moment of $\mu = 0 \text{ D}$, an ionization energy of $IE = 7.5 \text{ eV}$, and a diameter of 0.7 nm . Using these molecular parameters, estimate the Hamaker constant for condensed C_{60} .

Answer: The equation for the Hamaker constant can be simplified to:

$$A = -\pi \rho_A \rho_B C_w = -\pi (\rho_{C_{60}})^2 C_d$$

since molecular C_{60} is nonpolar and only London dispersion forces contribute to C_w . First, we transform the density of condensed C_{60} into a number density:

$$\begin{aligned} \rho_{C_{60}} &= \frac{\text{number of molecules}}{\text{volume}} \\ &= 1.65 \text{ g/cm}^3 \times \frac{6.02 \times 10^{23} \text{ molecules}}{(12.01 \text{ g})(60)} \times \frac{1 \text{ cm}^3}{10^{-6} \text{ m}^3} \\ &= 1.38 \times 10^{27} \text{ m}^{-3} \end{aligned}$$

We can then use the London equation to calculate C_d for two C_{60} molecules:

$$\begin{aligned} C_d &= -\frac{3\alpha^2 I}{4(4\pi\epsilon_0)^2} \\ &= -\frac{3}{4} (76.5 \times 10^{-30} \text{ m}^3)^2 (1.2 \times 10^{-18} \text{ J}) \\ &= -5.3 \times 10^{-75} \text{ J} \cdot \text{m}^6 \end{aligned}$$

Putting this altogether, we can calculate A as:

$$\begin{aligned} A &= -\pi \rho_A \rho_B C_w \\ &= -\pi (1.38 \times 10^{27} \text{ m}^{-3})^2 (-5.3 \times 10^{-75} \text{ J} \cdot \text{m}^6) \\ &= 3.2 \times 10^{-20} \text{ J} \end{aligned}$$

This value comes reasonably close to the value of the Hamaker constant ($7.5 \times 10^{-20} \text{ J}$) derived from experimental measurements of C_{60} interactions in water.

Worked Example 1.13

Question: Graphite is a layered solid that is held together only through vdW interactions. The Hamaker constant for graphite interacting across air is $A = 47 \times 10^{-20}$ J. Calculate the binding energy between two slabs of graphite separated by 1 nm.

Answer: Using Eq. 1.31, we calculate:

$$\begin{aligned} V_{surf-surf} &= \frac{-A}{12D^2} \text{ per unit area} \\ &= \frac{-47 \times 10^{-20} \text{ J}}{12(1 \times 10^{-9} \text{ m})^2} \\ &= -39 \times 10^{-3} \text{ J/m}^2 \end{aligned}$$

1.5 Hydrophobic Forces

Hydrophobic forces refer to the attraction between nonpolar molecules, particles, and surfaces in the presence of water. These hydrophobic (a word derived from the ancient Greek words for “water-fearing”) bodies experience a strong mutual attraction that is responsible for a wide range of phenomena, including the formation of surfactant micelles, cell membranes, and protein folding. This strong attraction often results in spontaneous ordering or *assembly* of hydrophobic molecules, as depicted for surfactants in Figure 1.30, such that water is expelled into the bulk.

However, unlike the intermolecular forces discussed in previous sections, there is no universal force law to describe the multitude of experimental observations that are attributed to hydrophobic forces. Hydrophobic forces have been observed to operate over both long-range (20–300 nm) and short-range (<20 nm). The derivation of a force law is also complicated by the knowledge that water molecules hydrate small versus large hydrophobic solutes in very different ways.

At the molecular scale, hydrophobic forces are attributed to the restructuring of H_2O molecules around hydrophobic solutes. In the bulk liquid state, H_2O has a strong tendency to form hydrogen bonds with four other neighboring H_2O molecules, giving rise to tetrahedral coordination (Figure 1.31). However, this coordination is *labile* since the lifetimes of these hydrogen bonds are short ($<10^{-11}$ s), allowing the intermolecular H_2O bonds to associate and dissociate rapidly. Hydrogen bond length in bulk liquid water also depends strongly on temperature and pressure. (It should be noted that there is still debate over what constitutes a “broken” hydrogen bond in water, as defined by either a critical bond length and/or bond angle.)

When a hydrophobic solute is introduced into liquid water, attractive forces between the solutes arise primarily due to a change in *entropy*. Let’s consider a simple hydrocarbon – an organic compound composed entirely of H and C atoms – such as the hexane molecule, C_6H_{14} , shown in Figure 1.32. To solvate hexane, H_2O molecules must break their tetrahedral coordination and reorganize to accommodate C_6H_{14} molecules. In effect, this forms a cavity in bulk water due to H_2O – H_2O hydrogen bond-breaking:

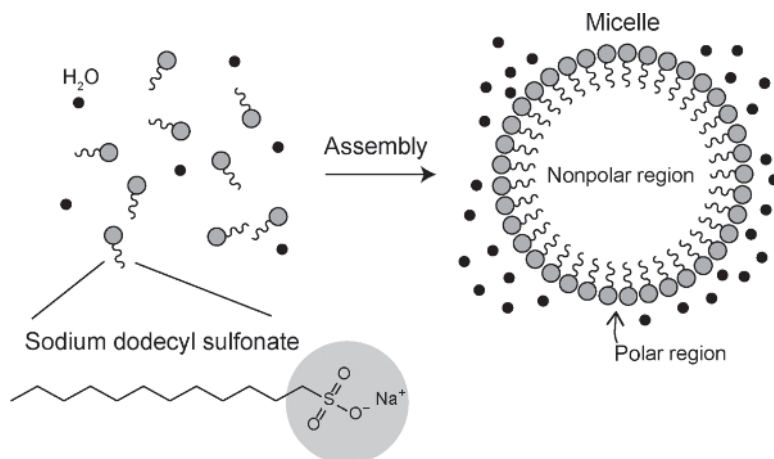
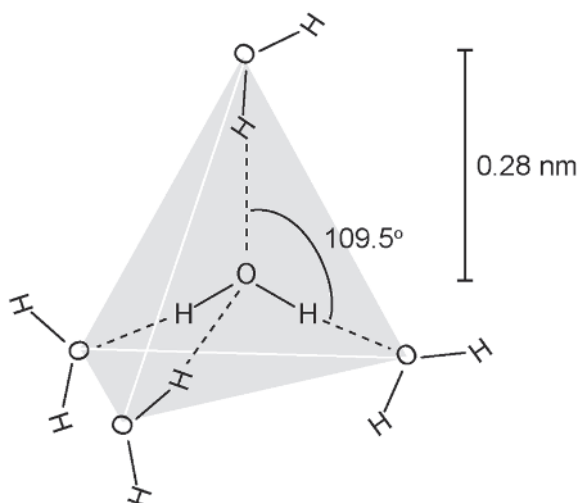


Figure 1.30 Surfactants such as sodium dodecyl sulfonate are amphiphilic molecules that can spontaneously order into spherical structures called micelles.

Figure 1.31 The tetrahedral structure of hydrogen-bonded water molecules in ice.



The H_2O molecules directly around the solute can compensate for this change in enthalpy (ΔH) by forming extra hydrogen bonds with its nearest H_2O neighbors to generate a cage-like H_2O structure. In our example, $\Delta H = 0 \text{ kJ/mol}$ for transferring a C_6H_{14} from a nonpolar solvent to water; in other words, there is no enthalpic cost for mixing hexane and water. However, the entropic cost for forming the ordered H_2O cage is significant ($\Delta S = 28 \text{ kJ/mol}$). The driving force for C_6H_{14} to self-segregate is the reduction in the number of H_2O molecules participating in these cage structures, which are entropically unfavored.

These short-range hydrophobic interactions are typically considered the main driving force for the formation of a variety of self-assembled structures, such as

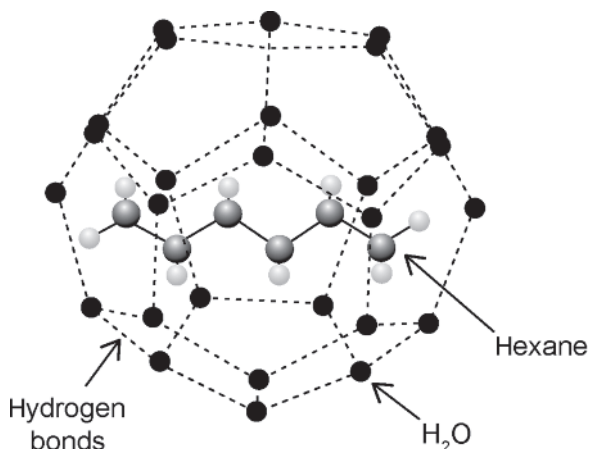


Figure 1.32 Water molecules form ordered, cage-like structures around nonpolar molecules like hexane.

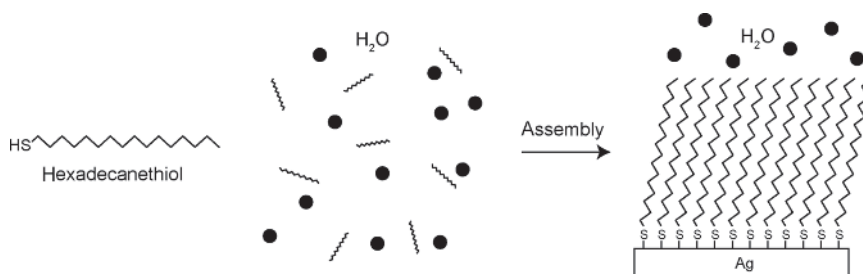


Figure 1.33 Self-assembled monolayers (SAMs) are formed by the spontaneous organization of alkanethiols in the presence of a metal surface, such as Ag or Au.

self-assembled monolayers (often abbreviated as SAMs) and *liposomes*. SAMs consist of molecules that organize into packed layers that are only a single-molecule thick (Figure 1.33). They are commonly used to passivate a variety of solid surfaces and nanoscale materials, such as metal nanoparticles, since the molecular monolayer forms a physical barrier against further chemical interactions or reactions. They typically comprise molecules that contain a hydrophobic component and a head group – a functional group located at the end of the molecule. The head group serves as a molecular anchor, forming a coordination or covalent bond to the solid surface. For example, alkanethiols are commonly used to form SAMs on metal Au and Ag surfaces. The thiol ($-\text{SH}$) head group serves as a *ligand* that deprotonates and binds to metal atoms to form a strong $\text{Au}-\text{S}$ or $\text{Ag}-\text{S}$ bond. However, the hydrophobic forces derived from the long alkane chain are the driving force for molecular organization into a dense hydrophobic layer.

Liposomes are an example of a self-assembled nanostructure that results largely from hydrophobic interactions (Figure 1.34). Liposomes are typically formed from phospholipids, the same molecules that comprise cell membranes:

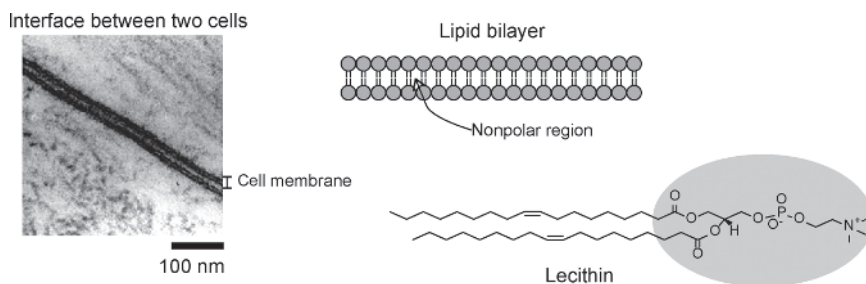


Figure 1.34 A transmission electron microscope image of the region where two cells touch (left). The dark regions show the electron-dense portion (circled, right) of the phospholipid comprising the cell membrane. Lecithin (right) is a representative phospholipid and a chief component of cell membranes.

While a cell membrane is considered a two-dimensional assembly of phospholipids, a liposome is a three-dimensional artificial vesicle that consists of fluid enclosed within a lipid bilayer (Figure 1.35). Unlike a micelle, a liposome possesses both hydrophilic interior and exterior surfaces. They are extensively used as encapsulants in the cosmetic and pharmaceutical industries because they can be employed to deliver both hydrophobic and hydrophilic molecules and because the phospholipid bilayer can be embedded with biological targeting groups. The liposome, similar to a SAM, forms a physical barrier around its contents that allow molecular payloads to be protected from oxidation and degradation processes.

While short-range hydrophobic interactions are relatively well understood, the fundamental mechanism behind long-range hydrophobic forces is still an active area of research. Long-range forces can be categorized as the attractive force that develops between hydrophobic surfaces, leading to phenomena such as the self-assembly of hydrophobic nanoparticles, with examples shown in Figure 1.36.

In some experimental cases, the observed attractions are not considered purely hydrophobic in nature and result from a combination of electrostatic and

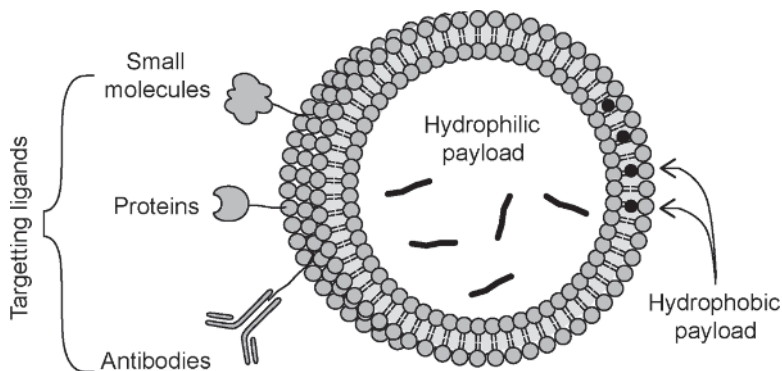


Figure 1.35 Liposomes are spherical structures composed of lipid bilayers. They can be used to encapsulate payloads in different regions and can be chemically modified to target specific biological entities.

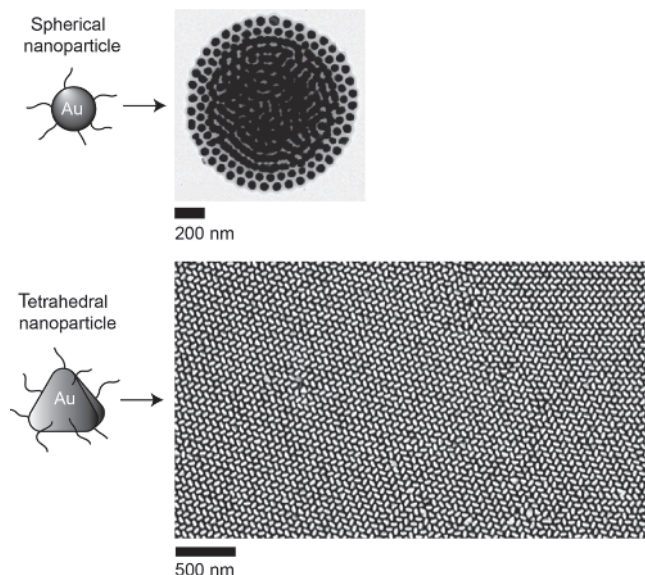


Figure 1.36 Au nanoparticles modified with hydrophobic ligands can undergo spontaneous self-organization into superstructure due to hydrophobic forces. Top: Spherical nanoparticle form nanoparticle micelles. Source: Reproduced from ACS Nano 2012, 6, 12, 11059–11065. Bottom: Hydrophobic tetrahedral nanocrystals form a herringbone superstructure. Source: Reproduced from J. Am. Chem. Soc. 2022, 144, 30, 13538–13546.

hydrophobic interactions that contribute to a long interaction distance. In other cases, it is proposed that H_2O molecules near the hydrophobic solute cause a local change in the Hamaker constant, enhancing the vdW interaction between hydrophobic surfaces by a significant amount. In the coming years, it is likely that advances in multiscale modeling – theoretical models that span multiple time and length scales – will pave the way in understanding how these various molecular-level effects contribute to long-range hydrophobic interactions and their corresponding phenomena.

1.6 Steric Forces

Steric repulsion results from the overlap in electron clouds for two approaching atoms or molecules at very short (interatomic, <1 nm) distances. This force can be both quantum–mechanical and electrostatic in nature. The quantum–mechanical component stems from the *Pauli exclusion principle*, which dictates that no two electrons share the same quantum state. The electrostatic component arises from *Born repulsion* between similarly charged electrons or from the repulsive interaction between two positively charged nuclei. As such, there is no universal force law that describes how steric interactions change with respect to distance. However, several empirical functions have been developed that adequately describe the behavior of this short-range repulsive potential.

One of the most well-known empirical functions is the *power-law potential*, of the form:

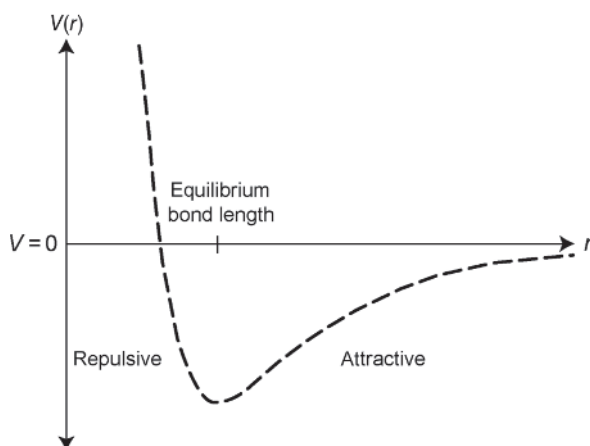
$$V = \left(\frac{\sigma}{r}\right)^n \quad (1.31)$$

where n is an integer usually between 9 and 16. The power-law potential is the form of the repulsive potential used in the Lennard-Jones or “6–12” potential:

$$V = \frac{A}{r^{12}} - \frac{B}{r^6} \quad (1.32)$$

where A and B are integers, and r is the intermolecular distance. The Lennard-Jones potential combines the attractive pair potential resulting from vdW interactions with a repulsive pair potential describing steric interactions. The total potential plotted in Figure 1.37 shows the appearance of a potential well:

Figure 1.37 The Lennard-Jones potential.



where energy is minimized at a separation distance that is typically associated with equilibrium bond length. The equilibrium bond length obtained for the Lennard-Jones potential can be used to determine the *van der Waals radius* of a molecule, which is defined as the radius of the imaginary hard sphere surrounding the molecule.

Worked Example 1.14

Question: C_{60} is a nonpolar molecule with no net charge, whose intermolecular interactions can be described by the Lennard-Jones potential (with constants $A = 34.8 \times 103 \text{ eV } \text{\AA}^{12}$ and $B = 20 \text{ eV } \text{\AA}^6$). Calculate the equilibrium bond length and binding energy for two C_{60} molecules in vacuum.

Answer: The pair potential between two C_{60} molecules is described by

$$V(r) = \frac{A}{r^{12}} - \frac{B}{r^6}$$

The bond length can be found by calculating the separation distance between the molecules at equilibrium, when the net force between two C_{60} molecules is zero:

$$\begin{aligned}
 F &= -\frac{dV(r)}{dr} = 0 \\
 &= \frac{d}{dr} \left(\frac{A}{r^{12}} - \frac{B}{r^6} \right) = \frac{-6A}{r^{11}} + \frac{6B}{r^5}
 \end{aligned}$$

Solving for r and substituting the Lennard-Jones constants, we get:

$$r = \left(\frac{2A}{B} \right)^{1/6} = \left(\frac{2 \cdot 34.8 \times 10^3 \text{ eV} \cdot \text{\AA}^{12}}{20 \text{ eV} \cdot \text{\AA}^6} \right)^{1/6} = 3.89 \text{ \AA}$$

To calculate the binding energy, we plug this value back into our equation for $V(r)$:

$$\begin{aligned}
 V(3.89 \text{ \AA}) &= \frac{34.8 \times 10^3 \text{ eV} \cdot \text{\AA}^{12}}{(3.89 \text{ \AA})^{12}} - \frac{20 \text{ eV} \cdot \text{\AA}^6}{(3.89 \text{ \AA})^6} \\
 &= -2.87 \text{ meV} \\
 &= -2.77 \text{ kJ/mol}
 \end{aligned}$$

Steric forces determine how close atoms and molecules can be situated from one another. This can have a profound effect on the chemical reactivity of molecules, nanomaterials, and surfaces. For example, steric *hindrance* occurs when chemical reactions are slowed due to the presence of bulky side groups or substituents of molecules. In chemical synthesis, steric hindrance can be engineered to block unwanted side reactions. In a similar manner, steric repulsion also has important

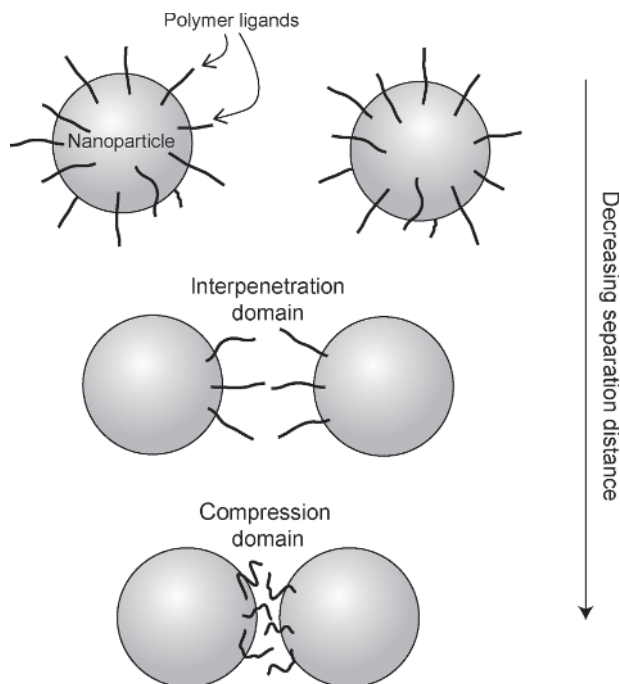


Figure 1.38 Polymer-grafted nanoparticle experience steric repulsion as they approach each other.

consequence for nanomaterials that are passivated by bulky molecules, such as polymers or SAMs. Molecular passivation layers control access to the surface, and thus contribute greatly to the thermodynamic, chemical, and physical properties of a nanomaterial.

Let us consider two nanoparticles that are grafted (i.e. chemically bound or anchored) with several polymer chains, as drawn in Figure 1.38. As the nanoparticles approach each other, they experience an increasing repulsive force due to steric overlap between the polymer chains that are trapped between the particles. This is usually described by two regions: (i) the interpenetration domain and (ii) the compression domain. The interpenetration domain is typically characterized by polymer–solvent interactions and occurs at interparticle distances of 1–2 polymer chain lengths. The compression domain occurs at shorter interparticle distances; in this regime, steric overlap causes the polymer grafts to adopt “compressed” configurations. This results in a decrease in the free volume – the unfilled void space associated with a molecule – of the polymer chains as the particles approach. This compression is entropically unfavorable and, thus, increases the free energy of the system. As a result, such nanoparticles are considered *entropically stabilized* because the polymer grafts generate this entropic steric repulsion upon close approach. The magnitude of this repulsive force is dependent on both the surface density and the free volume of the polymer grafts.

Worked Example 1.15

Question: Consider a dispersion of polymer-grafted nanoparticles in water that are stabilized mainly due to entropic interactions. How do you expect the aggregation state of these nanoparticles to change upon heating or cooling?

Answer: We can consider the overall Gibbs free energy of the nanoparticle system as

$$\Delta G = \Delta H - T\Delta S$$

where an increase or decrease in temperature modifies the entropic contribution in the second term. Heating the system increases the overall entropic contribution, and we would expect the nanoparticles to remain in a stable dispersion. Cooling decreases the overall entropic contribution and would likely destabilize the dispersion toward an aggregated or metastable state.

1.7 Particle Stability and Aggregation

Let us revisit our example of nanoparticles dispersed in a liquid medium from Figure 1.1. How do different intermolecular forces contribute to the behavior of such a nanoscale system? We can consider the case where our nanoparticles are subject to both repulsive *and* attractive interactions. The resulting pair potential would be the sum of multiple contributing pairwise potentials. The graphs in

Figure 1.39 show two very different cases that result from the addition of repulsive and attractive potential energy terms with varying magnitudes:

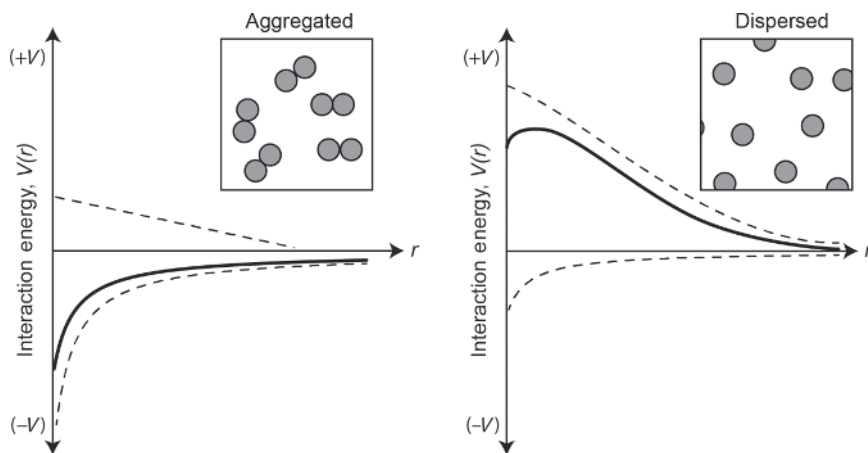


Figure 1.39 Two examples of pairwise potentials (solid line) that result from summing different repulsive and attractive interactions (dashed lines). A weak repulsive interaction leads to aggregated particles (left), while a weak attractive interaction leads to dispersed particles (right).

As we can see, the overall behavior of the nanoparticle dispersion will depend entirely on the relative strengths of the two forces at play. For the plot on the left, the pair potential exhibits a relatively weak repulsive interaction but a strong attractive interaction. Because the energy minimum occurs at $r = 0$, the nanoparticles will likely *aggregate* to form dimers or larger clusters. For the plot on the right, the pair potential exhibits a relatively strong repulsive interaction and only weak attraction. The minimum potential energy is achieved at $r \rightarrow \infty$; hence, the nanoparticles will stay suspended in the medium as a dispersed system.

In some cases, the pairwise potential exhibits multiple potential energy minima, such as the plot shown in Figure 1.40. These nanoparticle systems can exist in *metastable* states. For example, in the plot shown in Figure 1.40, the energy minimum occurs at $r = 0$. However, the nanoparticles may stay trapped in a local potential energy minimum by maintaining a separation distance greater than r_1 . For $r > r_1$, the potential energy is negative and stability is achieved as $r \rightarrow \infty$, even though it does not represent the absolute minimum energy that could be attained. This is often referred to as a metastable dispersion, since aggregation is limited by the energy barrier located at r_2 , depending on its height (ΔV). If ΔV is small, the particles will aggregate ($r \rightarrow 0$); if ΔV is large, the particles will stay dispersed ($r \rightarrow \infty$). ΔV is typically measured in units of thermal energy, $k_B T$ (where $k_B T = 4.11 \times 10^{-21}$ J at room temperature) and serves as a gauge for whether aggregation will occur.

Aggregation becomes an increasingly important consideration as particle size decreases. At the nanoscale, attractive vdW forces become competitive with steric

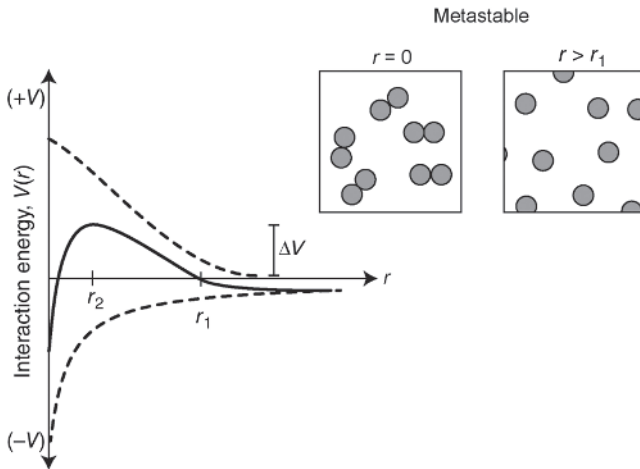


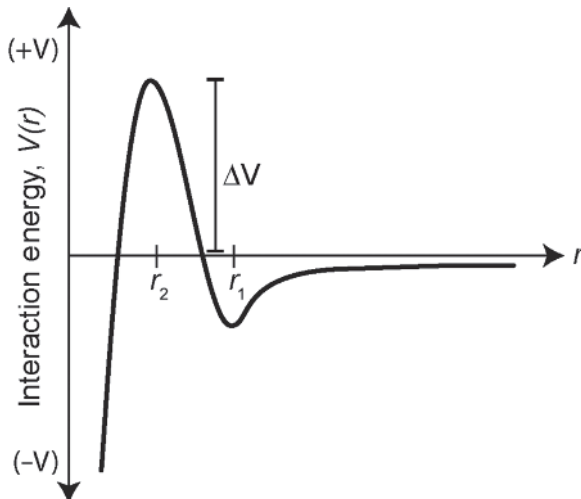
Figure 1.40 The sum of attractive and repulsive interactions (dashed lines) can lead to a pairwise potential that exhibits metastability.

and electrostatic repulsion, leading to different types of aggregation phenomena. This is not often the case for macroscopic objects (e.g. particles of sand), which require different long-range forces (such as gravity or capillary forces) to generate adhesion.

Worked Example 1.16

Question: Consider a dispersion of nanoparticles that exhibit the pairwise potential below (Figure 1.41). Describe the aggregation behavior of the nanoparticles for the two different cases: (i) $\Delta V \gg 0$ and for (ii) $\Delta V \approx 0$.

Figure 1.41 Possible pair potential for nanoparticles.



Answer: The pairwise potential above is characterized by an energy minimum at r_1 , an energy barrier at r_2 , and a deep energy well as r approaches 0. For case (i), the nanoparticles would likely come into stable equilibrium to form clusters with an interparticle separation distance of r_1 . The presence of a large energy barrier would cause the nanoparticles to remain kinetically stable at this separation distance. For case (ii), the nanoparticles would likely adhere into structures with a separation distance of r_1 (a metastable state) and then slowly aggregate.

Worked Example 1.17

Question: Two perfectly spherical silica (SiO_2) nanoparticles with a diameter of 30 nm are coated with a negatively charged surface coating and are separated by a distance of 5 nm. For what surface charge density does the repulsive electrostatic potential become equal but opposite to the attractive vdW potential?

Answer: First, we can calculate the pairwise potential for the vdW interaction between the two nanoparticles. From Table 1.2, we see that $A_{\text{SiO}_2} = 16.4 \times 10^{-20} \text{ J}$. Plugging this into the vdW expression for two interacting spheres, we get:

$$V = \frac{-AR}{12D} = \frac{-(16.4 \times 10^{-20} \text{ J})(15 \times 10^{-9} \text{ m})}{12(5 \times 10^{-9} \text{ m})} = -41 \times 10^{-21} \text{ J}$$

We can then plug this binding energy into the expression for electrostatic potential between two point charges to calculate the total charge, Q , for each nanoparticle. Recall that in this expression, r is the center-to-center distance between the particles.

$$V = \frac{Q^2}{4\pi\epsilon\epsilon_0 r} = 41 \times 10^{-21} \text{ J}$$

$$\frac{Q^2}{4\pi \left(8.85 \times 10^{-12} \frac{\text{C}^2}{\text{J} \cdot \text{m}} \right) (35 \times 10^{-9} \text{ m})} = 41 \times 10^{-21} \text{ J}$$

$$Q = -4.0 \times 10^{-19} \text{ C}$$

We can then plug this total charge into the equation for surface charge density, σ :

$$\sigma = \frac{Q}{A} = \frac{-4.0 \times 10^{-19} \text{ C}}{4\pi(15 \times 10^{-9} \text{ m})^2} = -1.4 \times 10^{-4} \text{ C/m}^2$$

To put this in context, this surface charge density is equivalent to one negative ion per every 1000 nm^2 or equivalently a rough separation distance of 30 nm on the surface of the nanoparticle.

Further Reading

Berg, J.C. (2010). *An Introduction to Interfaces & Colloids: The Bridge to Nanoscience*. World Scientific.

Hammer, M.U., Anderson, T.H., Chaimovich, A. et al. (2010). The search for the hydrophobic force law. *Faraday Discussions* 146: 299–308.

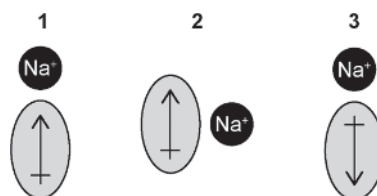
Israelachvili, J.N. (2011). *Intermolecular and Surface Forces*. Academic press.

- Rogers, B., Adams, J., and Pennathur, S. (2014). *Nanotechnology: Understanding Small Systems*. CRC Press.
- Silverstein, T.P. (1998). The real reason why oil and water don't mix. *Journal of Chemical Education* 75 (1): 116.
- Ulman, A. (2013). *An Introduction to Ultrathin Organic Films: From Langmuir-Blodgett to Self-Assembly*. Academic press.

Problems and Discussion Topics

- 1.1 List the intermolecular forces that you would expect to occur between ethanol ($\text{C}_2\text{H}_5\text{OH}$) and water (H_2O) molecules, in order of increasing strength.
- 1.2 List the following liquids in order of lowest to highest boiling points and briefly explain the reasoning behind your answer: H_2O , H_2S , H_2Se , and H_2Te .
- 1.3 List the following molecules in order of dipole moment, from smallest to largest: CO , CO_2 , CHCl_3 , C_6H_6 , and CH_3OH .
- 1.4 NH_3 has a dipole moment of 1.47 D. Consider the interaction energy between Na^+ and NH_3 in an aqueous solution with a separation distance of 0.2 nm ($\epsilon_{\text{H}_2\text{O}} = 80.10$). Calculate the interaction potential for each of the ion-dipole orientations shown below (Figure 1.42) and determine the orientation with the lowest potential energy.

Figure 1.42 Dipole-ion interactions.



- 1.5 If there is a uniformly spaced line of alternating anions and cations with a distance, d , between the centers of the ions, show that the interaction energy is given by:

$$E = \frac{\epsilon^2}{4\pi\epsilon_0} \frac{Z_A Z_B}{d} 2 \ln 2$$

- 1.6 Plot the interaction potential for a Na^+ ion and Cl^- ion as a function of separation distance in three different solvents:
 - (a) Water ($\epsilon = 80.2$)
 - (b) Ethylene glycol ($\epsilon = 37$)
 - (c) Chloroform ($\epsilon = 4.8$)

- 1.7** Calculate the Debye lengths and compare the screened electric fields, $V(r)$, for a nanoparticle dispersed in 10 mM CaCl_2 versus 10 mM MgSO_4 .
- 1.8** Calculate the Debye length for phosphate-buffered saline (PBS), which is a commonly used medium to mimic the physiological conditions of the human body. PBS is composed of the following electrolytes: 137 mM NaCl , 2.7 mM KCl , 10 mM Na_2HPO_4 , and 1.8 mM KH_2PO_4 . How does Debye screening in PBS impact nanoscale devices designed to go into the human body?
- 1.9** The electric polarizability of a fullerene molecule of C_{60} has been measured as 76.5 \AA^3 . Calculate the induced dipole moment, μ_{ind} , on C_{60} in the presence of a Na^+ ion located at a center-to-center distance of 2 nm away. How do you expect this value of μ_{ind} to compare to a molecule of methane (CH_3)? How about a carbon nanotube?
- 1.10** The pairwise potential in Figure 1.43 describes the aggregation behavior of positively charged nanoparticles dispersed in a NaCl solution.

Qualitatively plot how you would expect the pairwise potential to change under the following experimental conditions:

- Large increase in $[\text{NaCl}]$
- Large decrease in $[\text{NaCl}]$
- Change in electrolyte to CaCl_2 with equivalent molar concentration.

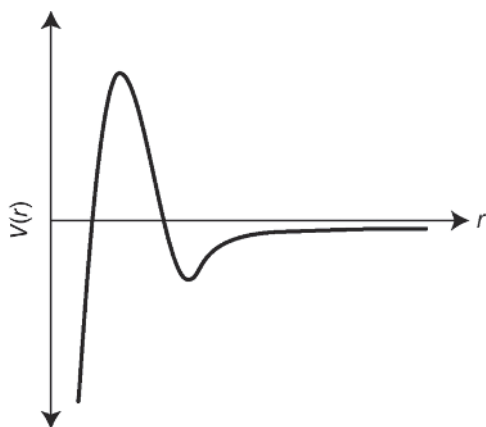


Figure 1.43 Possible pair potential for charged nanoparticles.

- 1.11** The heat of sublimation for Ne can be used to measure the bond dissociation energy for pure Ne, which is approximately 2 kJ/mol. Explain this discrepancy with the vdW pair potential for two Ne atoms calculated in the worked example.
- 1.12** Spontaneous opening of DNA's double helix structure to form single-stranded DNA is a rare event, but double-stranded DNA can be readily

“melted” to form single-stranded DNA by heating. Using your knowledge of base-pair interactions, formulate a simple expression for calculating the melting temperature of a DNA strand with a given sequence.

- 1.13** Derive the following expression for the induced dipole imparted by a polar molecule with a fixed orientation, ϑ , and dipole moment, μ , and a nonpolar molecule with polarizability, α , located at a separation distance of r :

$$\mu_{ind} = \frac{\mu\alpha\sqrt{(1 + 3\cos^2 \theta)}}{4\pi\epsilon\epsilon_0 r^3}$$

- 1.14** Consider a spherical particle with a radius, R , and a flat surface made of identical material separated at some distance, D , and held together only by vdW interactions. The *effective area of interaction* is defined as the area for which two flat surfaces at the same separation distance would have the same interaction force. Calculate the effective area of interaction of the spherical particle.
- 1.15** In a solution of polymer, a poor solvent can turn into a good solvent by increasing the temperature to a critical point called the *theta temperature*. Explain why miscibility is temperature dependent.
- 1.16** The bond strength of an H_2 molecule is 436 kJ/mol. The distance at which the bond breaks ($V = 0$) is 2.93 Å. Using the Lennard-Jones potential:
 (a) Calculate the equilibrium bond distance for H_2 .
 (b) Calculate the maximum adhesion force between the two H atoms.
- 1.17** For the Lennard-Jones potential, what is the predicted equilibrium separation distance for the minimum energy of interaction? What is the predicted separation distance when the adhesive force, F is maximum?
- 1.18** The diameter of C_{60} is 0.71 nm and the Lennard-Jones potential constants are $A = 34.8 \times 10^3 \text{ eV } \text{\AA}^{12}$ and $B = 20 \text{ eV } \text{\AA}^6$.
 (a) What are the intermolecular forces that drive fullerene crystallization?
 (b) Estimate the binding energy between two C_{60} molecules with a separation distance of 2 nm.
 (c) Do you expect the binding energy to be smaller or larger for two molecules of C_{70} ? Briefly explain your answer.
- 1.19** Stable dispersions of C_{60} in water can be obtained by modifying the C_{60} surface with negative charges. Calculate the surface charge required to separate two C_{60} molecules by a distance of 5 nm.
- 1.20** Films composed of crystallized C_{60} can be intercalated with Li^+ to serve as anodes for lithium-ion batteries. Li^+ ions have a radius of 6 Å. The diameter

of C_{60} is 0.71 nm and the Lennard-Jones potential constants are $A = 20 \text{ eV } \text{\AA}^6$ and $B = 34.8 \times 10^3 \text{ eV } \text{\AA}^{12}$.

- (a) Determine whether there is volume expansion in crystallized C_{60} when a Li^+ ion occupies the space between two C_{60} molecules.
- (b) The Hamaker constant for crystallized C_{60} is $4.02 \times 10^{-21} \text{ J}$. How do you expect the binding energy of solid C_{60} to change when Li^+ ions are introduced into the crystal? Briefly explain.

